PHYSICAL REVIEW D **71,** 051104(R) (2005)

Measurement of the forward-backward charge asymmetry from $W \to e\nu$ production in $p\bar{p}$ collisions at $\sqrt{s} = 1.96$ TeV

D. Acosta,[16] J. Adelman,[12] T. Affolder,[9] T. Akimoto,[54] M. G. Albrow,[15] D. Ambrose,[43] S. Amerio,[42] D. Amidei,[33] A. Anastassov,[50] K. Anikeev,[15] A. Annovi,[44] J. Antos,[1] M. Aoki,[54] G. Apollinari,[15] T. Arisawa,[56] J-F. Arguin,[32] A. Artikov,[13] W. Ashmanskas,[15] A. Attal,[7] F. Azfar,[41] P. Azzi-Bacchetta,[42] N. Bacchetta,[42] H. Bachacou,[28] W. Badgett,[15] A. Barbaro-Galtieri,[28] G. J. Barker,[25] V. E. Barnes,[46] B. A. Barnett,[24] S. Baroiant,[6] M. Barone,[17] G. Bauer,[31] F. Bedeschi,[44] S. Behari,[24] S. Belforte,[53] G. Bellettini,[44] J. Bellinger,[58] E. Ben-Haim,[15] D. Benjamin,[14] A. Beretvas,[15] A. Bhatti,[48] M. Binkley,[15] D. Bisello,[42] M. Bishai,[15] R. E. Blair,[2] C. Blocker,[5] K. Bloom,[33] B. Blumenfeld,[24] A. Bocci,[48] A. Bodek,[47] G. Bolla,[46] A. Bolshov,[31] P. S. L. Booth,[29] D. Bortoletto,[46] J. Boudreau,[45] S. Bourov,[15] B. Brau,[9] C. Bromberg,[34] E. Brubaker,[12] J. Budagov,[13] H. S. Budd,[47] K. Burkett,[15] G. Busetto,[42] P. Bussey,[19] K. L. Byrum,[2] S. Cabrera,[14] M. Campanelli,[18] M. Campbell,[33] A. Canepa,[46] M. Casarsa,[53] D. Carlsmith,[58] S. Carron,[14] R. Carosi,[44] M. Cavalli-Sforza,[3] A. Castro,[4] P. Catastini,[44] D. Cauz,[53] A. Cerri,[28] L. Cerrito,[23] J. Chapman,[33] C. Chen,[43] Y. C. Chen,[1] M. Chertok,[6] G. Chiarelli,[44] G. Chlachidze,[13] F. Chlebana,[15] I. Cho,[27] K. Cho,[27] D. Chokheli,[13] J. P. Chou,[20] M. L. Chu,[1] S. Chuang,[58] J. Y. Chung,[38] W-H. Chung,[58] Y. S. Chung,[47] C. I. Ciobanu,[23] M. A. Ciocci,[44] A. G. Clark,[18] D. Clark,[5] M. Coca,[47] A. Connolly,[28] M. Convery,[48] J. Conway,[6] B. Cooper,[30] M. Cordelli,[17] G. Cortiana,[42] J. Cranshaw,[52] J. Cuevas,[10] R. Culbertson,[15] C. Currat,[28] D. Cyr,[58] D. Dagenhart,[5] S. Da Ronco,[42] S. D'Auria,[19] P. de Barbaro,[47] S. De Cecco,[49] G. De Lentdecker,[47] S. Dell'Agnello,[17] M. Dell'Orso,[44] S. Demers,[47] L. Demortier,[48] M. Deninno,[4] D. De Pedis,[49] P. F. Derwent,[15] C. Dionisi,[49] J. R. Dittmann,[15] C. Dörr,[25] P. Doksus,[23] A. Dominguez,[28] S. Donati,[44] M. Donega,[18] J. Donini,[42] M. D'Onofrio,[18] T. Dorigo,[42] V. Drollinger,[36] K. Ebina,[56] N. Eddy,[23] J. Ehlers,[18] R. Ely,[28] R. Erbacher,[6] M. Erdmann,[25] D. Errede,[23] S. Errede,[23] R. Eusebi,[47] H-C. Fang,[28] S. Farrington,[29] I. Fedorko,[44] W. T. Fedorko,[12] R. G. Feild,[59] M. Feindt,[25] J. P. Fernandez,[46] C. Ferretti,[33] R. D. Field,[16] G. Flanagan,[34] B. Flaugher,[15] L. R. Flores-Castillo,[45] A. Foland,[20] S. Forrester,[6] G. W. Foster,[15] M. Franklin,[20] J. C. Freeman,[28] Y. Fujii,[26] I. Furic,[12] A. Gajjar,[29] A. Gallas,[37] J. Galyardt,[11] M. Gallinaro,[48] M. Garcia-Sciveres,[28] A. F. Garfinkel,[46] C. Gay,[59] H. Gerberich,[14] D. W. Gerdes,[33] E. Gerchtein,[11] S. Giagu,[49] P. Giannetti,[44] A. Gibson,[28] K. Gibson,[11] C. Ginsburg,[58] K. Giolo,[46] M. Giordani,[53] M. Giunta,[44] G. Giurgiu,[11] V. Glagolev,[13] D. Glenzinski,[15] M. Gold,[36] N. Goldschmidt,[33] D. Goldstein,[7] J. Goldstein,[41] G. Gomez,[10] G. Gomez-Ceballos,[10] M. Goncharov,[51] O. González,[46] I. Gorelov,[36] A. T. Goshaw,[14] Y. Gotra,[45] K. Goulianos,[48] A. Gresele,[4] M. Griffiths,[29] C. Grosso-Pilcher,[12] U. Grundler,[23] M. Guenther,[46] J. Guimaraes da Costa,[20] C. Haber,[28] K. Hahn,[43] S. R. Hahn,[15] E. Halkiadakis,[47] A. Hamilton,[32] B-Y. Han,[47] R. Handler,[58] F. Happacher,[17] K. Hara,[54] M. Hare,[55] R. F. Harr,[57] R. M. Harris,[15] F. Hartmann,[25] K. Hatakeyama,[48] J. Hauser,[7] C. Hays,[14] H. Hayward,[29] E. Heider,[55] B. Heinemann,[29] J. Heinrich,[43] M. Hennecke,[25] M. Herndon,[24] C. Hill,[9] D. Hirschbuehl,[25] A. Hocker,[47] K. D. Hoffman,[12] A. Holloway,[20] S. Hou,[1] M. A. Houlden,[29] B. T. Huffman,[41] Y. Huang,[14] R. E. Hughes,[38] J. Huston,[34] K. Ikado,[56] J. Incandela,[9] G. Introzzi,[44] M. Iori,[49] Y. Ishizawa,[54] C. Issever,[9] A. Ivanov,[47] Y. Iwata,[22] B. Iyutin,[31] E. James,[15] D. Jang,[50] J. Jarrell,[36] D. Jeans,[49] H. Jensen,[15] E. J. Jeon,[27] M. Jones,[46] K. K. Joo,[27] S. Jun,[11] T. Junk,[23] T. Kamon,[51] J. Kang,[33] M. Karagoz Unel,[37] P. E. Karchin,[57] S. Kartal,[15] Y. Kato,[40] Y. Kemp,[25] R. Kephart,[15] U. Kerzel,[25] V. Khotilovich,[51] B. Kilminster,[38] D. H. Kim,[27] H. S. Kim,[23] J. E. Kim,[27] M. J. Kim,[11] M. S. Kim,[27] S. B. Kim,[27] S. H. Kim,[54] T. H. Kim,[31] Y. K. Kim,[12] B. T. King,[29] M. Kirby,[14] L. Kirsch,[5] S. Klimenko,[16] B. Knuteson,[31] B. R. Ko,[14] H. Kobayashi,[54] P. Koehn,[38] D. J. Kong,[27] K. Kondo,[56] J. Konigsberg,[16] K. Kordas,[32] A. Korn,[31] A. Korytov,[16] K. Kotelnikov,[35] A. V. Kotwal,[14] A. Kovalev,[43] J. Kraus,[23] I. Kravchenko,[31] A. Kreymer,[15] J. Kroll,[43] M. Kruse,[14] V. Krutelyov,[51] S. E. Kuhlmann,[2] S. Kwang,[12] A. T. Laasanen,[46] S. Lai,[32] S. Lami,[48] S. Lammel,[15] J. Lancaster,[14] M. Lancaster,[30] R. Lander,[6] K. Lannon,[38] A. Lath,[50] G. Latino,[36] R. Lauhakangas,[21] I. Lazzizzera,[42] Y. Le,[24] C. Lecci,[25] T. LeCompte,[2] J. Lee,[27] J. Lee,[47] S. W. Lee,[51] R. Lefevre,[3] N. Leonardo,[31] S. Leone,[44] S. Levy,[12] J. D. Lewis,[15] K. Li,[59] C. Lin,[59] C. S. Lin,[15] M. Lindgren,[15] T. M. Liss,[23] A. Lister,[18] D. O. Litvintsev,[15] T. Liu,[15] Y. Liu,[18] N. S. Lockyer,[43] A. Loginov,[35] M. Loreti,[42] P. Loverre,[49] R-S. Lu,[1] D. Lucchesi,[42] P. Lujan,[28] P. Lukens,[15] G. Lungu,[16] L. Lyons,[41] J. Lys,[28] R. Lysak,[1] D. MacQueen,[32] R. Madrak,[15] K. Maeshima,[15] P. Maksimovic,[24] L. Malferrari,[4] G. Manca,[29] R. Marginean,[38] C. Marino,[23] A. Martin,[24] M. Martin,[59] V. Martin,[37] M. Martínez,[3] T. Maruyama,[54] H. Matsunaga,[54] M. Mattson,[57] P. Mazzanti,[4] K. S. McFarland,[47] D. McGivern,[30] P. M. McIntyre,[51] P. McNamara,[50] R. McNulty,[29] A. Mehta,[29] S. Menzemer,[31] A. Menzione,[44] P. Merkel,[15] C. Mesropian,[48] A. Messina,[49] T. Miao,[15] N. Miladinovic,[5] L. Miller,[20] R. Miller,[34] J. S. Miller,[33] R. Miquel,[28] S. Miscetti,[17] G. Mitselmakher,[16] A. Miyamoto,[26] Y. Miyazaki,[40] N. Moggi,[4] B. Mohr,[7] R. Moore,[15] M. Morello,[44] P. A. Movilla Fernandez,,[28] A. Mukherjee,[15] M. Mulhearn,[31] T. Muller,[25] R. Mumford,[24] A. Munar,[43] P. Murat,[15] J. Nachtman,[15] S. Nahn,[59] I. Nakamura,[43] I. Nakano,[39] A. Napier,[55] R. Napora,[24]

D. Naumov,[36] V. Necula,[16] F. Niell,[33] J. Nielsen,[28] C. Nelson,[15] T. Nelson,[15] C. Neu,[43] M. S. Neubauer,[8] C. Newman-Holmes,[15] T. Nigmanov,[45] L. Nodulman,[2] O. Norniella,[3] K. Oesterberg,[21] T. Ogawa,[56] S. H. Oh,[14] Y. D. Oh,[27] T. Ohsugi,[22] T. Okusawa,[40] R. Oldeman,[49] R. Orava,[21] W. Orejudos,[28] C. Pagliarone,[44] E. Palencia,[10] R. Paoletti,[44] V. Papadimitriou,[15] S. Pashapour,[32] J. Patrick,[15] G. Pauletta,[53] M. Paulini,[11] T. Pauly,[41] C. Paus,[31] D. Pellett,[6] A. Penzo,[53] T. J. Phillips,[14] G. Piacentino,[44] J. Piedra,[10] K. T. Pitts,[23] C. Plager,[7] A. Pompoš,[46] L. Pondrom,[58] G. Pope,[45] X. Portell,[3] O. Poukhov,[13] F. Prakoshyn,[13] T. Pratt,[29] A. Pronko,[16] J. Proudfoot,[2] F. Ptohos,[17] G. Punzi,[44] J. Rademacker,[41] M. A. Rahaman,[45] A. Rakitine,[31] S. Rappoccio,[20] F. Ratnikov,[50] H. Ray,[33] B. Reisert,[15] V. Rekovic,[36] P. Renton,[41] M. Rescigno,[49] F. Rimondi,[4] K. Rinnert,[25] L. Ristori,[44] W. J. Robertson,[14] A. Robson,[41] T. Rodrigo,[10] S. Rolli,[55] L. Rosenson,[31] R. Roser,[15] R. Rossin,[42] C. Rott,[46] J. Russ,[11] V. Rusu,[12] A. Ruiz,[10] D. Ryan,[55] H. Saarikko,[21] S. Sabik,[32] A. Safonov,[6] R. St. Denis,[19] W. K. Sakumoto,[47] G. Salamanna,[49] D. Saltzberg,[7] C. Sanchez,[3] A. Sansoni,[17] L. Santi,[53] S. Sarkar,[49] K. Sato,[54] P. Savard,[32] A. Savoy-Navarro,[15] P. Schlabach,[15] E. E. Schmidt,[15] M. P. Schmidt,[59] M. Schmitt,[37] L. Scodellaro,[10] A. L. Scott,[9] A. Scribano,[44] F. Scuri,[44] A. Sedov,[46] S. Seidel,[36] Y. Seiya,[40] F. Semeria,[4] L. Sexton-Kennedy,[15] I. Sfiligoi,[17] M. D. Shapiro,[28] T. Shears,[29] P. F. Shepard,[45] D. Sherman,[20] M. Shimojima,[54] M. Shochet,[12] Y. Shon,[58] I. Shreyber,[35] A. Sidoti,[44] J. Siegrist,[28] M. Siket,[1] A. Sill,[52] P. Sinervo,[32] A. Sisakyan,[13] A. Skiba,[25] A. J. Slaughter,[15] K. Sliwa,[55] D. Smirnov,[36] J. R. Smith,[6] F. D. Snider,[15] R. Snihur,[32] A. Soha,[6] S. V. Somalwar,[50] J. Spalding,[15] M. Spezziga,[52] L. Spiegel,[15] F. Spinella,[44] M. Spiropulu,[9] P. Squillacioti,[44] H. Stadie,[25] B. Stelzer,[32] O. Stelzer-Chilton,[32] J. Strologas,[36] D. Stuart,[9] A. Sukhanov,[16] K. Sumorok,[31] H. Sun,[55] T. Suzuki,[54] A. Taffard,[23] R. Tafirout,[32] S. F. Takach,[57] H. Takano,[54] R. Takashima,[22] Y. Takeuchi,[54] K. Takikawa,[54] M. Tanaka,[2] R. Tanaka,[39] N. Tanimoto,[39] S. Tapprogge,[21] M. Tecchio,[33] P. K. Teng,[1] K. Terashi,[48] R. J. Tesarek,[15] S. Tether,[31] J. Thom,[15] A. S. Thompson,[19] E. Thomson,[43] P. Tipton,[47] V. Tiwari,[11] S. Tkaczyk,[15] D. Toback,[51] K. Tollefson,[34] T. Tomura,[54] D. Tonelli,[44] M. Tönnesmann,[34] S. Torre,[44] D. Torretta,[15] S. Tourneur,[15] W. Trischuk,[32] J. Tseng,[41] R. Tsuchiya,[56] S. Tsuno,[39] D. Tsybychev,[16] N. Turini,[44] M. Turner,[29] F. Ukegawa,[54] T. Unverhau,[19] S. Uozumi,[54] D. Usynin,[43] L. Vacavant,[28] A. Vaiciulis,[47] A. Varganov,[33] E. Vataga,[44] S. Vejcik III,[15] G. Velev,[15] V. Veszpremi,[46] G. Veramendi,[23] T. Vickey,[23] R. Vidal,[15] I. Vila,[10] R. Vilar,[10] I. Vollrath,[32] I. Volobouev,[28] M. von der Mey,[7] P. Wagner,[51] R. G. Wagner,[2] R. L. Wagner,[15] W. Wagner,[25] R. Wallny,[7] T. Walter,[25] T. Yamashita,[39] K. Yamamoto,[40] Z. Wan,[50] M. J. Wang,[1] S. M. Wang,[16] A. Warburton,[32] B. Ward,[19] S. Waschke,[19] D. Waters,[30] T. Watts,[50] M. Weber,[28] W. C. Wester III,[15] B. Whitehouse,[55] A. B. Wicklund,[2] E. Wicklund,[15] H. H. Williams,[43] P. Wilson,[15] B. L. Winer,[38] P. Wittich,[43] S. Wolbers,[15] C. Wolfe,[12] M. Wolter,[55] M. Worcester,[7] S. Worm,[50] T. Wright,[33] X. Wu,[18] F. Würthwein,[8] A. Wyatt,[30] A. Yagil,[15] C. Wang,[59] U. K. Yang,[12] W. Yao,[28] G. P. Yeh,[15] K. Yi,[24] J. Yoh,[15] P. Yoon,[47] K. Yorita,[56] T. Yoshida,[40] I. Yu,[27] S. Yu,[43] Z. Yu,[59] J. C. Yun,[15] L. Zanello,[49] A. Zanetti,[53] I. Zaw,[20] F. Zetti,[44] J. Zhou,[50] A. Zsenei,[18] and S. Zucchelli[4]

(CDF Collaboration)

[1]*Institute of Physics, Academia Sinica, Taipei, Taiwan 11529, Republic of China*
[2]*Argonne National Laboratory, Argonne, Illinois 60439, USA*
[3]*Institut de Fisica d'Altes Energies, Universitat Autonoma de Barcelona, E-08193, Bellaterra (Barcelona), Spain*
[4]*Istituto Nazionale di Fisica Nucleare, University of Bologna, I-40127 Bologna, Italy*
[5]*Brandeis University, Waltham, Massachusetts 02254, USA*
[6]*University of California at Davis, Davis, California 95616, USA*
[7]*University of California at Los Angeles, Los Angeles, California 90024, USA*
[8]*University of California at San Diego, La Jolla, California 92093, USA*
[9]*University of California at Santa Barbara, Santa Barbara, California 93106, USA*
[10]*Instituto de Fisica de Cantabria, CSIC-University of Cantabria, 39005 Santander, Spain*
[11]*Carnegie Mellon University, Pittsburgh, Pennsylvania 15213, USA*
[12]*Enrico Fermi Institute, University of Chicago, Chicago, Illinois 60637, USA*
[13]*Joint Institute for Nuclear Research, RU-141980 Dubna, Russia*
[14]*Duke University, Durham, North Carolina 27708*
[15]*Fermi National Accelerator Laboratory, Batavia, Illinois 60510, USA*
[16]*University of Florida, Gainesville, Florida 32611, USA*
[17]*Laboratori Nazionali di Frascati, Istituto Nazionale di Fisica Nucleare, I-00044 Frascati, Italy*
[18]*University of Geneva, CH-1211 Geneva 4, Switzerland*
[19]*Glasgow University, Glasgow G12 8QQ, United Kingdom*
[20]*Harvard University, Cambridge, Massachusetts 02138, USA*

[21]*The Helsinki Group: Helsinki Institute of Physics, FIN-00014, Helsinki, Finland; and Division of High Energy Physics, Department of Physical Sciences, University of Helsinki, FIN-00014, Helsinki, Finland*
[22]*Hiroshima University, Higashi-Hiroshima 724, Japan*
[23]*University of Illinois, Urbana, Illinois 61801, USA*
[24]*The Johns Hopkins University, Baltimore, Maryland 21218, USA*
[25]*Institut für Experimentelle Kernphysik, Universität Karlsruhe, 76128 Karlsruhe, Germany*
[26]*High Energy Accelerator Research Organization (KEK), Tsukuba, Ibaraki 305, Japan*
[27]*Center for High Energy Physics: Kyungpook National University, Taegu 702-701, Korea; Seoul National University, Seoul 151-742, Korea; and SungKyunKwan University, Suwon 440-746, Korea*
[28]*Ernest Orlando Lawrence Berkeley National Laboratory, Berkeley, California 94720, USA*
[29]*University of Liverpool, Liverpool L69 7ZE, United Kingdom*
[30]*University College London, London WC1E 6BT, United Kingdom*
[31]*Massachusetts Institute of Technology, Cambridge, Massachusetts 02139, USA*
[32]*Institute of Particle Physics: McGill University, Montréal, Canada H3A 2T8; and University of Toronto, Toronto, Canada M5S 1A7*
[33]*University of Michigan, Ann Arbor, Michigan 48109, USA*
[34]*Michigan State University, East Lansing, Michigan 48824, USA*
[35]*Institution for Theoretical and Experimental Physics (ITEP), Moscow 117259, Russia*
[36]*University of New Mexico, Albuquerque, New Mexico 87131, USA*
[37]*Northwestern University, Evanston, Illinois 60208, USA*
[38]*The Ohio State University, Columbus, Ohio 43210, USA*
[39]*Okayama University, Okayama 700-8530, Japan*
[40]*Osaka City University, Osaka 588, Japan*
[41]*University of Oxford, Oxford OX1 3RH, United Kingdom*
[42]*Istituto Nazionale di Fisica Nucleare, Sezione di Padova-Trento, University of Padova, I-35131 Padova, Italy*
[43]*University of Pennsylvania, Philadelphia, Pennsylvania 19104, USA*
[44]*Istituto Nazionale di Fisica Nucleare, University and Scuola Normale Superiore of Pisa, I-56100 Pisa, Italy*
[45]*University of Pittsburgh, Pittsburgh, Pennsylvania 15260, USA*
[46]*Purdue University, West Lafayette, Indiana 47907, USA*
[47]*University of Rochester, Rochester, New York 14627, USA*
[48]*The Rockefeller University, New York, New York 10021, USA*
[49]*Istituto Nazionale di Fisica Nucleare, Sezione di Roma 1, University di Roma "La Sapienza", I-00185 Roma, Italy*
[50]*Rutgers University, Piscataway, New Jersey 08855, USA*
[51]*Texas A&M University, College Station, Texas 77843, USA*
[52]*Texas Tech University, Lubbock, Texas 79409, USA*
[53]*Istituto Nazionale di Fisica Nucleare, University of Trieste/Udine, Italy*
[54]*University of Tsukuba, Tsukuba, Ibaraki 305, Japan*
[55]*Tufts University, Medford, Massachusetts 02155, USA*
[56]*Waseda University, Tokyo 169, Japan*
[57]*Wayne State University, Detroit, Michigan 48201, USA*
[58]*University of Wisconsin, Madison, Wisconsin 53706, USA*
[59]*Yale University, New Haven, Connecticut 06520, USA*
(Received 10 January 2005; published 31 March 2005)

We report a measurement of the forward-backward charge asymmetry of electrons from W boson decays in $p\overline{p}$ collisions at $\sqrt{s} = 1.96$ TeV using a data sample of 170 pb^{-1} collected by the Collider Detector at Fermilab. The asymmetry is measured as a function of electron rapidity and transverse energy and provides new input on the momentum fraction dependence of the u and d quark parton distribution functions within the proton.

DOI: 10.1103/PhysRevD.71.051104 PACS numbers: 13.38.Be, 13.85.Qk, 14.60.Cd, 14.70.Fm

I. INTRODUCTION

A necessary input for cross section calculations at a hadron collider is an estimate of the momentum distribution of the incoming partons that participate in the hard-scattering process. The probability of finding a parton carrying momentum fraction x within the incoming hadron is expressed in the parton distribution function (PDF). At the Tevatron, any cross section calculation will have to integrate over the proton and antiproton PDFs. Presently, many measurements at the Tevatron have significant uncertainties associated with the choice of PDF. These uncertainties will become more important as the data sets continue to grow. For example, PDF uncertainty is expected to be among the dominant systematic uncertainties in a precision determination of the W boson mass.

The PDFs are not calculable and must be determined using measurements from a wide range of scattering processes [1,2]. Measurement of the forward-backward charge

asymmetry in $p\overline{p} \rightarrow W^{\pm} + X$ provides important input on the ratio of the u and d quark components of the PDF. Since u quarks carry, on average, a higher fraction of the proton momentum than d quarks [3], a W^+ produced by $u\bar{d} \rightarrow W^+$ tends to be boosted forward, in the proton direction. Similarly, a W^- tends to be boosted backward. This results in a nonzero forward-backward charge asymmetry defined as

$$A(y_W) = \frac{d\sigma(W^+)/dy_W - d\sigma(W^-)/dy_W}{d\sigma(W^+)/dy_W + d\sigma(W^-)/dy_W}, \qquad (1)$$

where y_W is the rapidity of the W bosons and $d\sigma(W^{\pm})/dy_W$ is the differential cross section for W^+ or W^- boson production.

Leptonic decays of the W boson, in our case $W \rightarrow e\nu$, provide a high purity sample for measuring this asymmetry. However, because p_Z of the neutrino is unmeasured, y_W is not directly determined, and we instead measure

$$A(\eta_e) = \frac{d\sigma(e^+)/d\eta_e - d\sigma(e^-)/d\eta_e}{d\sigma(e^+)/d\eta_e + d\sigma(e^-)/d\eta_e}, \qquad (2)$$

where η_e is the electron pseudorapidity [4]. By assuming the $W \rightarrow e\nu$ decays are described by the Standard Model $V - A$ couplings, $A(\eta_e)$ probes the PDF.

Previous measurements of the asymmetry [5], using 110 pb^{-1} of $p\overline{p}$ data at $\sqrt{s} = 1.8$ TeV collected by the Collider Detector at Fermilab (CDF), have provided constraints on the PDFs for u and d quarks at momentum transfer of $Q^2 \approx M_W^2$. In this article we describe a new measurement based on data collected with the CDF II detector at $\sqrt{s} = 1.96$ TeV corresponding to an integrated luminosity of 170 pb^{-1}. We measure the asymmetry in two regions of electron E_T that probe different ranges of y_W and thus increase sensitivity to the PDFs in the region $x > 0.3$ where currently they are least constrained.

II. DETECTOR DESCRIPTION

The CDF II detector [6] has undergone a major upgrade since the previous data-taking period. The components relevant to this measurement are described here.

Tracking detectors immersed within a 1.4 T solenoidal magnetic field are used to reconstruct the trajectories (tracks) and measure the momentum of charged particles. The Central Outer Tracker (COT) is a 3.1 m long open-cell drift chamber which provides track measurements (hits) in 96 layers in the radial range 40 cm $< r <$ 137 cm [7]. Closer to the beam, a silicon tracking system [8] provides precise hits from eight layers of sensors spanning 1.3 cm $< r <$ 28 cm and extending up to 1.8 m along the beam line. The COT allows track reconstruction in the range $|\eta| \lesssim 1$. The silicon detector extends that range to $|\eta| \lesssim 2.5$.

Segmented electromagnetic (EM) and hadronic calorimeters surround the tracking system and measure the energy of particles [9]. The energy of electrons is measured by lead-scintillator sampling calorimeters. In the central region, $|\eta| < 1.1$, the calorimeters are arranged in a projective barrel geometry and measure EM energy with a resolution of $[\sigma(E_T)/E_T]^2 = (13.5\%)^2/E_T(\mathrm{GeV}) + (2\%)^2$. In the forward region, $1.2 < |\eta| < 3.5$, the calorimeters are arranged in a projective "end-plug" geometry and measure EM energy with a resolution of $[\sigma(E_T)/E_T]^2 = (14.4\%)^2/E_T(\mathrm{GeV}) + (0.7\%)^2$.

Both central and forward EM calorimeters are instrumented with finely segmented detectors which measure shower position at a depth where energy deposition by a typical shower reaches its maximum. In the central region we use proportional wire chambers with cathode strip readout; in the forward region shower position is measured by two layers of 5 mm wide scintillating strips with a stereo angle of 45 degrees between them.

III. DATA SETS AND SELECTION

Our signal sample is comprised of $W \rightarrow e\nu$ candidate events, and a sample of $Z^0 \rightarrow e^+e^-$ candidate events is used to calibrate the charge identification. Events of interest are initially selected by an online trigger system with differing requirements for the central and forward regions. For W candidates, the central trigger requires an EM energy cluster with $E_T > 18$ GeV and a matching track with $p_T > 9$ GeV/c. To avoid any potential charge bias in the track trigger efficiency, we also accept events from a trigger which requires an EM energy cluster with $E_T >$ 20 GeV and missing transverse energy ($\not\!\!E_T$) of at least 25 GeV, but has no explicit track requirement. The forward trigger for W candidates requires an EM energy cluster with $E_T > 20$ GeV and $\not\!\!E_T > 15$ GeV. A backup trigger drops the $\not\!\!E_T$ requirement and is used to estimate the QCD jet background contribution. The trigger for Z candidates requires two EM energy clusters with $E_T > 18$ GeV.

The criteria used to identify the electron and positron candidates, which are described in detail in Ref. [10] and summarized below, are designed to reject the energy deposits from photons or QCD jets.

(i) $E_T > 25$ GeV.

(ii) $F_{\mathrm{Iso}} < 0.1$, where $F_{\mathrm{Iso}} \equiv$ additional energy in an "isolation" cone, of angular radius $R = \sqrt{(\Delta\phi)^2 + (\Delta\eta)^2} = 0.4$ centered on the electron, divided by the electron energy.

(iii) It is required that the associated hadronic energy is less than 5% of the EM energy.

(iv) The shower shape in the EM calorimeter and shower maximum detector must be consistent with that observed from test-beam data.

(v) The position along the beam line of the $p\overline{p}$ collision, z_0, is well reconstructed and $|z_0| < 60$ cm [11].

(vi) A track consistent with the position and energy measured in the calorimeter is required.

COT tracks, reconstructed independent of the calorimeter measurement, can be compared to it in position and

momentum. However, the coverage of the COT is limited to $|\eta| \lesssim 1$. To extend the measurement to higher $|\eta|$, we instead use silicon tracks reconstructed by a new calorimeter-seeded algorithm as described below. Two points and a signed curvature define a unique helix. The positions of the electromagnetic shower and of the $p\overline{p}$ collision provide the two points. The curvature of the trajectory is predicted from the transverse energy measured by the calorimeter. These two points and the curvature are used to generate two seed helices and associated covariance matrices, one for each charge hypothesis. Those seed helices are then projected into the silicon detector where hits are attached using a road-based search and requiring at least 4 attached hits with $\chi^2/\mathrm{dof} < 8$. If silicon tracks are fit for both charge hypotheses, the χ^2/dof is used to identify the charge with the best fit, and cases with $\Delta\chi^2/\mathrm{dof} < 0.5$ are rejected as ambiguous.

The relative alignment of the silicon detector and the calorimeter is determined using a sample of well identified $e^{\pm}$ with both COT and silicon tracks. To avoid a charge bias from the W charge asymmetry, we explicitly equalize the number of events of each charge used in the alignment for $\eta > 0$ and separately for $\eta < 0$. Offsets of $\mathcal{O}(1\ \mathrm{mm})$ and rotations of $\mathcal{O}(10\ \mathrm{mrad})$ are measured and corrected. The resulting position resolution in the forward calorimeter is measured to be 1 mrad, consistent with the design expectation.

Candidate $W \rightarrow e\nu$ events are required to have exactly one such $e^{\pm}$ candidate as well as $\not\!\!E_T > 25$ GeV and transverse mass in the range $50\ \mathrm{GeV}/c^2 < M_T < 100\ \mathrm{GeV}/c^2$. To suppress backgrounds from QCD and Drell-Yan processes, we require that there be no other EM energy depositions with $E_T > 25$ GeV. The selected sample contains 49 124 central and 28 806 forward events.

IV. MEASUREMENT OF THE CHARGE ASYMMETRY

Directly measured in the experiment and shown in Fig. 1 is the raw, uncorrected, asymmetry. In order to reconstruct $A(\eta_e)$, the measurement needs to be corrected for the effects of charge misidentification and background contributions. These η dependent corrections are applied bin-by-bin, and binning coarser than shown in Fig. 1 is used to reduce the effect of the uncertainty from these corrections.

A. Charge misidentification

The electron identification is constructed, and observed, to have a charge symmetric efficiency. However, resolution effects can lead to misidentification of the charge, which dilutes the asymmetry. Residual misalignments in the silicon detector and calorimeters could give rise to a bias in the charge identification that would directly bias the asymmetry. We measure the probability of such misidentification and correct for it. Calling that probability f_+ for e^+ and f_- for e^-, the corrected asymmetry can be computed from the raw asymmetry as $A = (A_{\mathrm{raw}} + f_+ - f_-)/(1 - f_+ - f_-)$.

We measure $f_{\pm}(\eta)$ with $Z^0 \rightarrow e^+e^-$ events where a track matched to one lepton tags the charge of the other. The tagging leg must have $|\eta| < 1.5$, and COT track information is used if it is available. The average misidentification probability i.e., without distinguishing between e^+ and e^-, is shown as a function of η in Fig. 2. The difference between the misidentification probability for e^+ and e^- is shown in Fig. 3,

B. Background corrections

We correct the measurement for the contributions of three sources of background: QCD jets, $Z^0 \rightarrow e^+e^-$, and $W \rightarrow \tau\nu \rightarrow e\nu\nu\nu$.

The background contribution from QCD jets faking the $W \rightarrow e\nu$ signature is measured by comparing the isolation of the $e^{\pm}$ candidate to the $\not\!\!E_T$ in the event [10]. Electrons from W decays tend to be isolated, i.e., have low F_{iso} values, while background from QCD jets have larger values. Similarly, $W \rightarrow e\nu$ events have large $\not\!\!E_T$ while QCD jets have lower values. If there is no correlation between

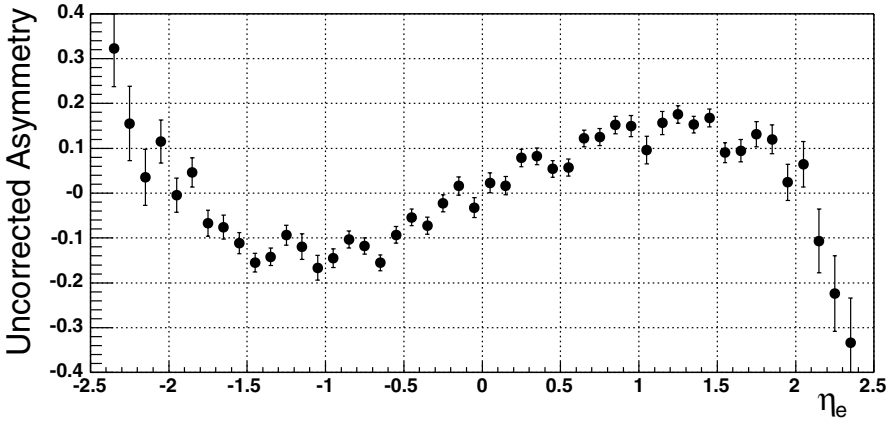

FIG. 1. The raw, uncorrected, charge asymmetry is plotted as a function of electron η.

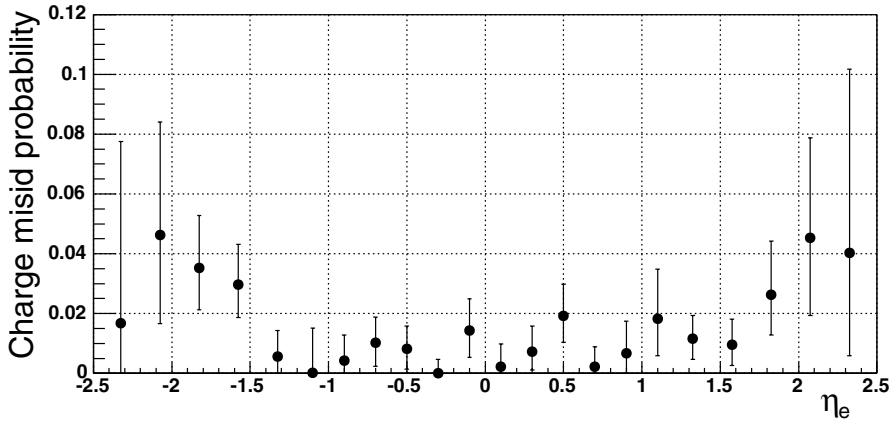

FIG. 2. The charge misidentification probability is plotted as a function of electron η.

isolation and $\not\!\!E_T$ for QCD jets, we can measure their shapes in the non-W regions and extrapolate them into the signal region. Studies of these variables demonstrate that they are not correlated if the selection requirements related to the EM shower shape are relaxed. Including those requirements suppresses events with high values of $F_{\rm iso}$, which makes the extrapolation statistically imprecise and degrades our ability to measure any potential correlation, so we remove them in estimating the QCD jet background. That results in an overestimate of the background, but it yields a statistically and systematically robust estimate. This measured upper bound on the background fraction is 2% for $|\eta| < 1$ and increases to about 15% for $|\eta| > 2$. We correct the raw asymmetry by a factor of $1 + F_{\rm QCD}$, where for the background fraction $F_{\rm QCD}$ we use half the measured upper bound, with uncertainties of $\pm 50\%$. Since we have only an upper limit, this choice provides full coverage of the actual value at 2σ.

$Z^0 \rightarrow e^+e^-$ events in which one of the leptons is lost represent a small, but asymmetric background [12]. This background contribution is determined with a Monte Carlo calculation using the PYTHIA generator[13], and it corresponds to about 1% of the signal. $W \rightarrow \tau\nu \rightarrow e\nu\nu\nu$ events bias the measured asymmetry because the τ decay dilutes the information available in the $e^{\pm}$ direction. This background contribution is about 4% of the signal. The number of e^+ and e^- events predicted for these backgrounds are subtracted from the measured values bin-by-bin in η.

Figure 4 shows the fully corrected $A(\eta_e)$.

C. E_T dependence

The asymmetry probes a large range of x for the parent u and d quarks, from an upper value of approximately 0.5, where valence quarks dominate, down to 2×10^{-3}, where sea quarks dominate. Large values of y_W correspond to the extreme values of x. For example, a high-x u quark and a low-x $\bar{d}$ quark lead to W^+ with large p_Z and therefore large y_W. The $V - A$ couplings in the $W \rightarrow e\nu$ decay cause the e^+ to be preferentially emitted opposite the W^+ flight direction. The electron asymmetry, $A(\eta_e)$, is a convolution of these competing production and decay asymmetries, which results in the sign change of $A(\eta_e)$ at large $|\eta_e|$.

Direct sensitivity to the PDF would be improved by reducing the decay asymmetry effect, e.g., by reconstructing the W direction. The unmeasured p_Z of the neutrino and the poor $\not\!\!E_T$ resolution complicate this reconstruction.

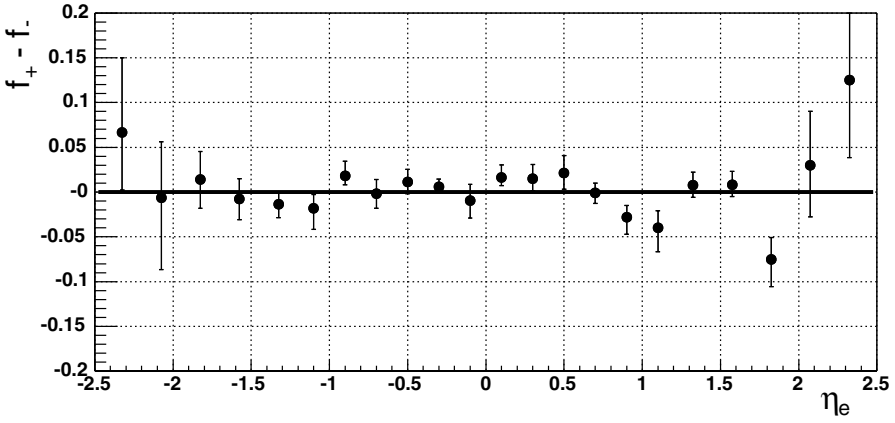

FIG. 3. The difference in charge misidentification probability of e^+ and e^-, $f_+(\eta) - f_-(\eta)$, is plotted as a function of electron η.

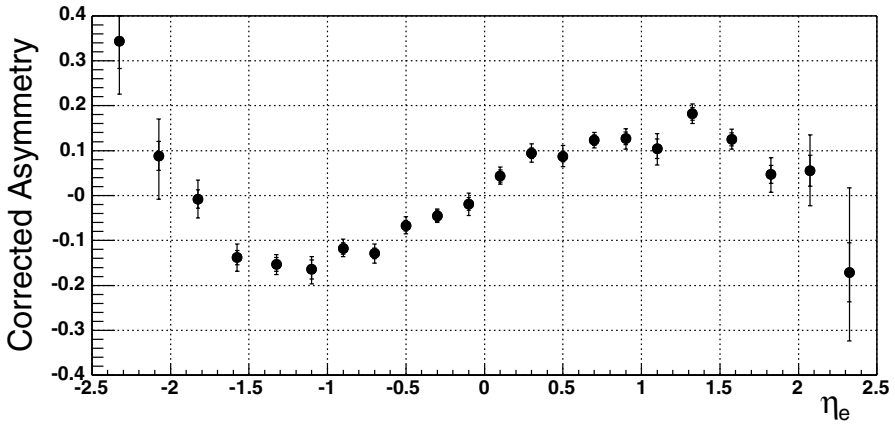

FIG. 4. The fully corrected charge asymmetry is plotted as a function of electron η. Both statistical and total (statistical + systematic) uncertainties are shown.

However, we can improve the correspondence between η_e and y_W based on the kinematics of just the electron, which is well measured. The neutrino p_Z ambiguity is a smaller effect for electrons with high E_T than for those at low E_T. We exploit this by separating the asymmetry measurement into bins of electron E_T. The size of the statistical and systematic uncertainties allows two bins, 25 GeV $< E_T <$ 35 GeV and 35 GeV $< E_T <$ 45 GeV. For a given η_e, the two E_T regions probe different ranges of y_W, and therefore x, and the higher E_T bin corresponds to a narrower range. As a result, measuring the asymmetry separately in the two bins allows a finer probe of the x dependence.

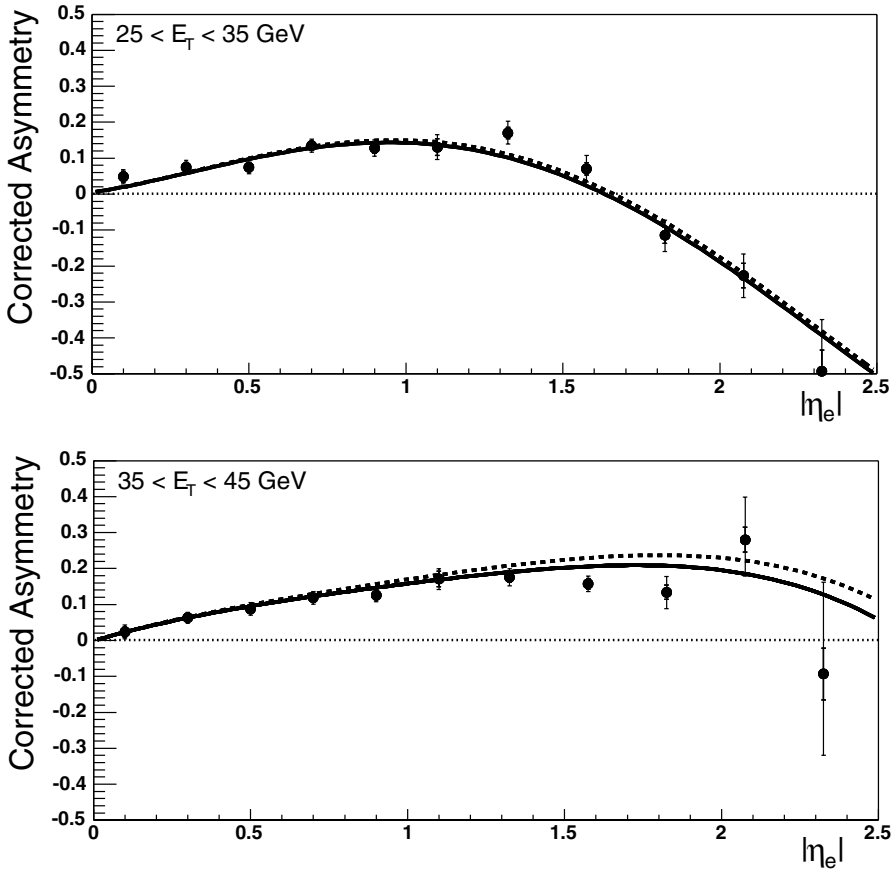

FIG. 5. The measured asymmetry, $A(|\eta_e|)$, is plotted and predictions from the CTEQ6.1M (solid) and MRST02 (dashed) PDFs are compared using a NLO RESBOS calculation. Both statistical and total (statistical + systematic) uncertainties are shown. The upper plot is for $25 < E_T < 35$ GeV. The lower plot is for $35 < E_T < 45$ GeV.

D. Systematic uncertainties

The corrections for charge misidentification and background contributions are measured and applied separately for each E_T bin since they are E_T dependent. The statistical uncertainty on the charge misidentification correction dominates the systematic uncertainty on the asymmetry measurement. The uncertainty from the QCD jet background correction is small, and the other background uncertainties are negligible.

Detector misalignments can induce an inherent charge bias. Such biases would be naturally corrected by the charge misidentification probabilities measured from the data. Nonetheless, we check the robustness of the charge determination by varying the alignment corrections within their uncertainties and verifying that the resulting changes in the asymmetry are not significant. We also verify that using COT tracks, when they are available, instead of silicon tracks results in no significant difference.

CP invariance requires $A(-\eta_e) = -A(\eta_e)$. The fully corrected data shown in Fig. 4 show no evidence of *CP* asymmetry; the level of agreement is characterized by $\chi^2/\mathrm{dof} = 9.5/11$. The $\pm\eta_e$ data are folded together to obtain a more precise measure of $A(|\eta_e|)$.

These results are most useful as input to future global PDF fits. Such fits use Monte Carlo generators without a full detector simulation. We have studied possible biases introduced by detector effects by comparing the asymmetry from a PYTHIA Monte Carlo generator to the fully simulated results and found no significant effects.

E. Results

The measured asymmetry $A(|\eta_e|)$ is listed in Table I and plotted in Fig. 5 for the two E_T regions. Predictions from CTEQ [1] and MRST [2] PDFs, which fit to previous CDF results [5], are shown for comparison. Those predictions use a NLO RESBOS Monte Carlo calculation with soft gluon resummation to model the W p_T distribution, to which they can be sensitive [14]. Since the previous measurements upon which these predictions are based are least constraining for $|\eta| > 1$ and do not separate the E_T dependence, inclusion of our results will further constrain future fits and improve the predictions.

TABLE I. The measured asymmetry values are tabulated in percent with combined statistical and systematic uncertainties. The listed $|\eta_e|$ is the event weighted average. Asymmetric uncertainties listed for some values arise because of the Poisson and binomial statistics inherent in the event counting.

$\lvert\eta_e\rvert$	$A(\lvert\eta_e\rvert)$		
	$E_T > 25$	$25 < E_T < 35$	$35 < E_T < 45$
0.11	$3.4^{+1.6}_{-1.5}$	4.8 ± 2.0	2.3 ± 1.9
0.30	6.2 ± 1.2	7.5 ± 1.9	6.3 ± 1.5
0.50	7.5 ± 1.5	7.5 ± 1.9	8.8 ± 1.8
0.70	12.6 ± 1.3	13.5 ± 1.8	11.8 ± 1.7
0.89	$12.2^{+1.6}_{-1.4}$	12.8 ± 2.3	$12.6^{+1.7}_{-1.9}$
1.09	13.8 ± 2.3	13.1 ± 3.5	17.1 ± 2.9
1.33	16.8 ± 1.6	$17.0^{+3.4}_{-3.0}$	17.6 ± 2.4
1.57	13.0 ± 1.8	$7.0^{+3.8}_{-3.6}$	15.7 ± 2.2
1.81	2.9 ± 2.9	$-11.5^{+4.2}_{-4.5}$	$13.4^{+4.4}_{-4.6}$
2.04	$-0.4^{+6.2}_{-5.7}$	-23 ± 6	28^{+12}_{-10}
2.31	-29 ± 10	-49 ± 14	-9^{+26}_{-23}

ACKNOWLEDGMENTS

We thank the Fermilab staff and the technical staffs of the participating institutions for their vital contributions. We thank Pavel Nadolsky for providing the RESBOS predictions. This work was supported by the U.S. Department of Energy and National Science Foundation; the Italian Istituto Nazionale di Fisica Nucleare; the Ministry of Education, Culture, Sports, Science and Technology of Japan; the Natural Sciences and Engineering Research Council of Canada; the National Science Council of the Republic of China; the Swiss National Science Foundation; the A.P. Sloan Foundation; the Bundesministerium fuer Bildung und Forschung, Germany; the Korean Science and Engineering Foundation and the Korean Research Foundation; the Particle Physics and Astronomy Research Council and the Royal Society, U.K.; the Russian Foundation for Basic Research; the Comision Interministerial de Ciencia y Tecnologia, Spain; in part by the European Community's Human Potential Programme under Contract No. HPRN-CT-20002, Probe for New Physics.

[1] J. Pumplin, D. R. Stump, J. Huston, H. L. Lai, P. Nadolsky, and W. K. Tung, J. High Energy Phys. 07 (2002) 012.

[2] A. Martin, R. Roberts, W. Stirling, and R. Thorne, Eur. Phys. J. C **4**, 463 (1998).

[3] H. L. Lai *et al.*, Phys. Rev. D **51**, 4763 (1995).

[4] We use a cylindrical coordinate system about the beam axis in which z is the proton direction, θ is the polar angle, ϕ is the azimuthal angle, and pseudorapidity $\eta \equiv -\ln\tan(\theta/2)$ is an excellent approximation for the rapidity of low mass particles. $E_T \equiv E\sin\theta$ and $p_T \equiv p\sin\theta$ where E is energy measured by the calorimeter and p is momentum measured by the spectrometer. The transverse momentum of the neutrino can be inferred from the missing transverse energy, $\not\!\!E_T \equiv -\sum_i E_T^i \mathbf{n}_i$, where $\mathbf{n}_i$ is the unit vector in the azimuthal plane that points from the beam line to the center of the ith calorimeter tower. The

transverse mass, M_T, measures the invariant mass using only momentum and energy transverse to the beam direction.

[5] F. Abe *et al.*, Phys. Rev. Lett. **81**, 5748 (1998).

[6] CDF II Collaboration, R. Blair *et al.*, FERMILAB-PUB-96-390-E, 1996.

[7] CDF II Collaboration, A. Affolder *et al.*, Nucl. Instrum. Methods Phys. Res., Sect. A **526**, 249 (2004).

[8] A. Sill *et al.*, Nucl. Instrum. Methods Phys. Res., Sect. A **447**, 1 (2000);A. Affolder *et al.*, Nucl. Instrum. Methods Phys. Res., Sect. A **453**, 84 (2000).

[9] L. Balka *et al.*, Nucl. Instrum. Methods Phys. Res., Sect. A **267**, 272 (1988);M. Albrow *et al.*, Nucl. Instrum. Methods Phys. Res., Sect. A **480**, 524 (2002).

[10] CDF II Collaboration, D. Acosta *et al.*, Phys. Rev. Lett. **94**, 091803 (2005).

[11] The z_0 position is found by vertexing all the other tracks from the $p\overline{p}$ interaction. If more than one interaction point is found, we use the one with the largest associated p_T, estimated as the scalar Σp_T of all tracks used in the vertex fit.

[12] CDF II Collaboration, D. Acosta *et al.*, hep-ex/0411059 [Phys. Rev. D (to be published)].

[13] T. Sjöstrand *et al.*, Comput. Phys. Commun. **135**, 238 (2001).

[14] F. Landry, R. Brock, P. M. Nadolsky, and C. P. Yuan, Phys. Rev. D **67**, 073016 (2003).